JOURNAL OF
EMERGING INVESTIGATORS

Article

Examination of the rotation curve for the dark matter deficient relic galaxy NGC 1277

Marina Alioto[1], Ignasi Pérez-Ràfols[2*], Santi Roca-Fàbrega[3*], Tyler Alioto[4,5]
[1] Institut Moisès Broggi, Barcelona, Spain
[2] Departament de Física, EEBE, Universitat Politècnica de Catalunya, Barcelona, Spain
[3] Lund Observatory, Division of Astrophysics, Department of Physics, Lund University, Lund, Sweden
[4] Centro Nacional de Análisis Genómico (CNAG), Barcelona, Spain
[5] Universitat de Barcelona (UB), Barcelona, Spain
These authors contributed equally to this work.

SUMMARY

Most galaxies exhibit flat rotation curves, indicating the presence of dark matter. However, recent observations reveal outlier galaxies exhibiting more Keplerian rotation curves, suggesting they have negligible amounts of dark matter. Here we reexamine the galactic kinematics of relic galaxy NGC 1277, a galaxy recently identified as deficient in dark matter, through a reproduction of the rotation curve, using data from the George and Cynthia Mitchell Spectrograph. We hypothesized that its galactic rotation curve could be used on its own to closely model its mass distribution. However, we calculate a total mass of 5.8×10^{10} $M_\odot$ within five effective radii, three times lower than the current predicted mass, showing that rotation curves do not account for all mass within a specified orbit. To understand the difference between our result and previous results, we consider different sources of error in our computation, such as inclination angle, bulge-disk geometry, velocity dispersion, and the possibility of an over-massive black hole. Our study shows how the shape of a rotation curve of a compact lenticular galaxy is not as closely dependent on its dark matter fraction as previously assumed, as well as the importance of modelling its shape and stellar composition for determination of its mass distribution. This has important implications for the utility of rotation curves for the discovery of additional galaxies with anomalous dark matter fractions.

INTRODUCTION

Rotation curves have played an important role in the discovery of dark matter and the development of matter distribution models in galaxies (1). A rotation curve describes the rotational velocities of a sample of stars as a function of their radial distance to the center of the galaxy. According to Kepler's third law, which states that the square of a planet's orbital period (T) is proportional to the cube of its average orbital radius (r) or $T^2 \propto r^3$, objects orbiting a center of gravity at a greater distance should orbit more slowly than those within smaller orbits. Although Kepler's third law applies to planetary motion, when applied to stellar rotation in galaxies, it leads to predictions that diverge from observation. The observation of "flat" rotation curves, indicating a more or less constant velocity in outer orbiting stars, was key in Vera Rubin's discovery of dark matter; an excess of undetectable matter further from the center of the galaxy was needed to explain why these stars would orbit at such high velocities (Figure 1) (2).

The term "escape velocity" is used to refer to the velocity an orbiting object needs to reach to leave the system. Typically, this term is applied to satellites of planets or planets within a solar system. The equation for escape velocity,

$$v = \sqrt{\frac{2GM}{r}} \qquad \text{(Equation 1)}$$

where G is the gravitational constant and r is the distance to the central massive object, relies heavily on the mass of the central object M (i.e. the mass of the planet or the mass of the star). For stars around a galaxy, however, the observed velocities of single stars or groups of stars depend on the total mass (e.g. black holes, stellar mass, and dark matter) contained within their orbits. However, the observed velocity of stars exceeds the escape velocities predicted for visible matter, which is the key observation leading to the theory of dark matter. If there were no dark matter, the stars in outer orbits would exceed the escape velocity. In other words, the mass around which the outermost stars or star clusters orbit would essentially reach a limit, increasing relatively little, and, given the formula above, r should reflect a characteristic Keplerian inverse proportionality, resulting in a decrease in velocity proportional to the increase in radius.

In 1914, Slipher discovered that the Andromeda "nebula" (now known as galaxy M31) rotates, and by 1917, Francis Pease calculated a constant angular velocity for the central region (3, 4). In the 1930s, based on these and additional calculations, several studies inferred the total mass of M31 and discussed its unexpectedly high mass-to-light ratio (M/L ratio) (5–7), suggesting the existence of some kind of non-luminous matter. In 1933, Fritz Zwicky studied the velocity dispersion of galaxies in the Coma cluster and coined the term "dark matter" to explain why visible mass could not account for the system's gravitational binding (8). However, it was not until the 1970s that the existence of additional matter in some galaxies was explicitly argued as the result of the discrepancy in outer regions of the galaxies between the photometric data (apparent luminosity of the stars and respective density) and the kinetic energy of the stars (derived from spectral

https://doi.org/10.59720/25-050

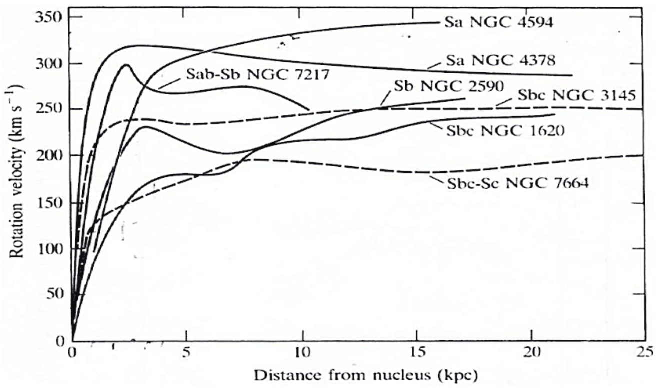

Figure 1: Series of rotation curves for spiral galaxies. Rotational velocities in km/s for seven galaxies as a function of their distance from the nucleus in kpc. Curves were smoothed to minimize variations across spiral arms and remove small differences between measurements from opposite sides of each nucleus. Galaxies are prefixed with their Hubble type. Curves for NGC3145 and NGC7664 are the "flattest" and are plotted with dashed lines. Reproduced with permission from Rubin, Ford, and Thonnard, et al. 1978 (2).

data using the 21 cm Hydrogen absorption lines). Several authors confirmed flat rotation curves of many galaxies out to the largest radius observed (Figure 1), concluding that the largest radii cannot be assumed to be the edge of the galaxy. Therefore, spiral galaxies must extend further than their apparent luminous size based on star and gas distribution (2, 9). By 1978, work by Albert Bosma proved the extension of galaxies beyond their optical size, and Vera Rubin provided the first persuasive evidence of dark matter by analyzing the kinematics of ten spiral galaxies, all of which presented flat rotation curves (2).

However, while the necessity of dark matter to fit standard gravitational models is acknowledged, there is no agreement on what this dark matter could be. Proposed candidates include subatomic particles (such as neutrinos, weakly interacting massive particles [WIMPs], and axions), brown dwarfs, neutron stars or primordial black holes (10–16). To better understand the nature of dark matter, there has been a recent focus on galaxies exhibiting unusual distributions of dark matter. Since the Hubble Space Telescope (HST) observations of dark matter deficient galaxy NGC 1052-DF2 in 2018, growing observations of galaxies deficient in dark matter, including the model dark matter deficient galaxies NGC 1277 (Figure 2) and FCC 224, have made them an evident yet unresolved mystery (17, 18). Possible explanations for the apparent lack of dark matter in NGC 1277 include that it was born with little dark matter; lost it during its "blue nugget" phase due to cluster interactions; formed from high-velocity gas collisions where baryons remained but dark matter escaped; or, more generally, that dark matter was removed through tidal stripping as proposed for other dark matter deficient galaxies (19–21).

Focusing on the characteristics of these anomalous dark matter deficient galaxies promises to shed some much-needed light on dark matter. While current cosmological simulations predict that in relic galaxies with masses similar to NGC 1277, the dark matter fraction (DMF) should vary from about 15% in the first effective radius (R_e, also known as the half-light radius, the radius within which a specific astronomical object, such as a galaxy or globular cluster, emits half of its total luminosity) up to approximately 60% within five R_e, Comerón, et al. report a DMF of only 1.8% within five R_e (22). Here we have chosen to re-analyze the rotation curve of NGC 1277. The rotation curve is a logical simplified calculation that has been crucial in the discovery of dark matter, which can explain the tension between the observed flattening of rotation curves and the kinematic curves predicted by Kepler's laws. It follows that the rotation curve of galaxies with low DMF should better fit the ideal Keplerian curve, allowing one to model their mass distribution and determine total enclosed mass (also known as integral mass) more closely. Here we determine the rotation curve of NGC 1277, which shows that stellar velocities peak at three kiloparsecs (kpc) from the galaxy center and then decrease. The enclosed mass appears to plateau at this point as well, suggesting an insignificant effect of dark matter in these outer orbits. However, contrary to our expectations, our estimation of total enclosed mass, or dynamical mass, at five R_e (five times the half-light radius) is substantially lower than our estimate for luminous or stellar mass. We conclude that rotation curves may still help detect dark matter deficient galaxies but cannot on their own be utilized to directly estimate the DMF.

RESULTS

To plot the rotation curve of NGC 1277, we used the kinematics previously derived from spectroscopic data from the George and Cynthia Mitchell Spectrograph (GCMS, 26). The shape of NGC 1277's rotation curve (Figure 3) does not appear to plateau as rotation curves characteristically do, indicative of the effect of dark matter in the outer parts of the galaxy. Instead, the data shows that objects reach a maximum velocity of 248±4 km/s approximately 3 kpc from the center and, as the Kepler model would predict, decrease with additional distance, indicating the possible deficiency of dark matter. Additional data points beyond 6 kpc would provide additional support for this trend; however, the spectrographic data corresponding to these points proved less reliable and

Figure 2: Image of NGC 1277 in the Perseus Cluster. The main image is 31 arcmin across (about 2 million light-years); Inset image is 1 arcmin across (about 64,000 light-years). RA Position: 03:19:51.482. Dec. Position: +41:34:24.902. Original image by Hubble Space Telescope, NASA, ESA (47). HST data obtained from program 14215 (48).

JOURNAL OF
EMERGING INVESTIGATORS

https://doi.org/10.59720/25-050

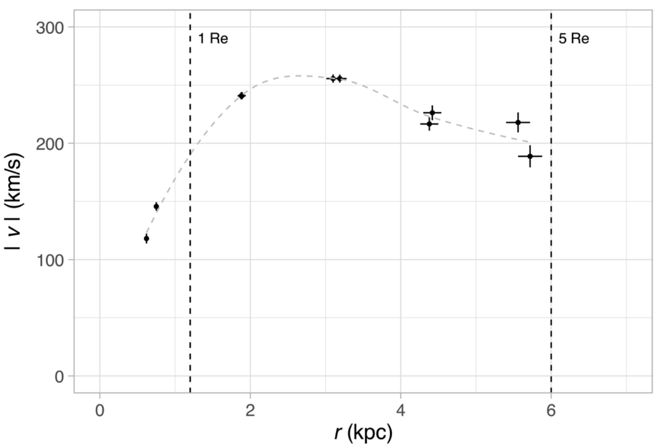

Figure 3: Rotation curve of NGC 1277. Rotational velocity of the selected data (Table 1) plotted as a function of their distance r (computed from original x and y coordinates) relative to the galactic center of NGC 1277. The trendline (gray dashed line) was calculated using the loess local regression function in R v4.4.2 with default parameters. The distances corresponding to o1 R_e (1.2 kpc) and 5 R_e (6 kpc) are indicated with vertical dashed lines.

was excluded due to any one of the following criteria: either signal to noise ratio was too low (<7), kinematic error was too high (>65 km/s), or velocity dispersion was outside a reasonable range (10 km/s to 350 km/s) (22).

We then studied the mass distribution in NGC 1277 by equating the centripetal and gravitational forces. From our calculations (Table 1), we deduced a relationship between mass and distance by fitting the data to a logarithmic function (Figure 4). The square of the coefficient of determination (R^2) describes a good fit of the data to the regression model, with a value of 0.942.

$$M_r\,[M_\odot] = 1.26 \times 10^{10} + 2.55 \times 10^{10} \ln\left(r[1\,kpc]\right) \qquad \text{(Equation 2)}$$

Taking the equation of the function (Equation 2), an interpolation of galactic mass (measured in $M_\odot$ a function of radial distance (r), we use logarithmic interpolation and extrapolation to determine that the mass enclosed within $1R_e$ (1.2 kpc) is (1.7 ± 0.2)×10^{10} $M_\odot$, and the mass enclosed within $5R_e$ (6 kpc) is (5.8 ± 0.3)×10^{10} $M_\odot$.

Finding the fraction of dark matter making up the total mass of NGC 1277 is synonymous with finding the difference between total dynamical mass, calculated above, and baryonic mass, the latter being "normal" matter comprised of stars, dust and gas, planets, etc., in addition to the black hole mass (estimated at 5×10^9 $M_\odot$) (26). To find the stellar mass, the major component of normal baryonic matter in early type galaxies, we calculated the total luminosity, from which we derived a total stellar mass of 1.4×10^{11} $M_\odot$. Our estimate of the dynamical mass of 5.8×10^{10} $M_\odot$ (95% CI = 5.3–6.3×10^{10} $M_\odot$) within a radius of 6 kpc falls well short of both our predicted stellar mass of 1.4×10^{11} $M_\odot$ based on photometric data and the more rigorously estimated value of 1.8×10^{11} $M_\odot$ for the total mass of NGC 1277 which used Jeans Anisotropic MGE (JAM) modeling to incorporate both the surface brightness profiles and the stellar kinematics to generate a best-fit total mass model (22). Therefore, the difference between dynamical and baryonic mass becomes negative, rendering a negative DMF, which does not make physical sense.

DISCUSSION

Using experimental kinematic data from the George and Cynthia Mitchell Spectrograph, we calculated a rotation curve for the dark matter deficient relic galaxy NGC 1277. This confirmed a decrease in velocity as a function of distance that appears to follow the inverse relationship given by Kepler's third law, which suggests the lack of a dark matter halo. However, the dynamical mass that we estimated using the rotation curve is approximately one third of the previously reported total galaxy mass of 1.8×10^{11} $M_\odot$, which was estimated assuming a Salpeter initial mass function (presence of many redder low-mass stars) and took into account both stellar velocity and dispersion and a high mass-to-light ratio (22). Our initial assumption that the kinetic data alone, as analyzed through the rotation curve and mass-to-radius graph, accounts for all the mass within the orbits corresponding to the radii, is inaccurate for NGC 1277: our simple calculation does not incorporate the full complexity of current galactic models.

It is possible that our own calculations of the rotation curve, and estimation of enclosed mass based on it, were sensitive to the limited range and precision of the spectrographic

x (arcsec)	y (arcsec)	r (kpc)	v(km/s)	v_{corr} (km/s)	M_r ($M_\odot$)	M_{r_corr} ($M_\odot$)
1.61	0.76	0.62 ± 0.02	-114.6 ± 4.1	-118.1 ± 4.2	(1.9 ± 0.2) × 10^9	(2.0 ± 0.2) × 10^9
-1.74	-1.26	0.75 ± 0.02	141.4 ± 3.6	145.7 ± 3.7	(3.5 ± 0.3) × 10^9	(3.7 ± 0.3) × 10^9
5.21	-1.24	1.88 ± 0.05	-233.6 ± 3.0	-240.8 ± 3.1	(2.4 ± 0.1) × 10^{10}	(2.5 ± 0.1) × 10^{10}
-5.34	0.74	1.89 ± 0.05	233.7 ± 3.0	240.9 ± 3.1	(2.4 ± 0.1) × 10^{10}	(2.6 ± 0.1) × 10^{10}
8.8	0.56	3.10 ± 0.09	-248.0 ± 3.5	-255.6 ± 3.6	(4.4 ± 0.2) × 10^{10}	(4.7 ± 0.3) × 10^{10}
-8.98	-1.34	3.19 ± 0.09	248.0 ± 3.4	255.6 ± 3.5	(4.6 ± 0.3) × 10^{10}	(4.8 ± 0.3) × 10^{10}
12.4	-1.44	4.4 ± 0.1	-210.2 ± 5.6	-216.6 ± 5.8	(4.5 ± 0.4) × 10^{10}	(4.8 ± 0.4) × 10^{10}
-12.58	0.66	4.4 ± 0.1	219.5 ± 6.2	226.2 ± 6.4	(5.0 ± 0.4) × 10^{10}	(5.3 ± 0.4) × 10^{10}
15.84	0.61	5.6 ± 0.2	-211.4 ± 8.3	-217.9 ± 8.6	(5.8 ± 0.6) × 10^{10}	(6.1 ± 0.7) × 10^{10}
-16.24	-1.45	5.7 ± 0.2	183.2 ± 9.2	188.8 ± 9.5	(4.5 ± 0.6) × 10^{10}	(4.7 ± 0.6) × 10^{10}

Table 1: Radius, velocity, and estimated enclosed galaxy mass for the ten fibers whose center is within the restricted radius. The estimated galactic center is located at the origin (0,0) and x,y coordinates are relative to the galactic center given in arcsec. Velocity v and estimated enclosed galaxy mass M_r are shown without correction for inclination angle and with correction: velocity v_{corr} = v/sin(76°), which accounts for the inclination angle. Galaxy mass estimations, in solar masses, are derived from rotational curve (radii and rotational velocities) by applying Equation 3.

https://doi.org/10.59720/25-050

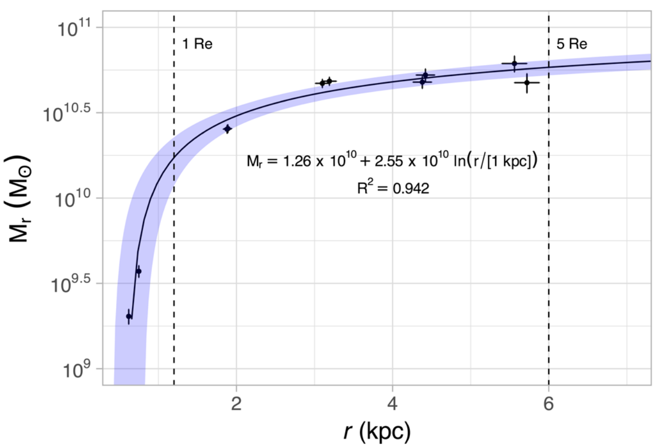

Figure 4: Integral mass of the galaxy enclosed within a given radius. The fitted logarithmic function is plotted as a solid black line, with the 95% confidence interval plotted as a blue ribbon. Error bars represent standard error in both radial distance and mass enclosed within that radius.

measurements. The original spectrographic data from the GCMS with sufficient quality extends out to 6 kpc while the galaxy extends to perhaps 10-12 kpc. We cannot be certain that the rotation curve will continue to fall according to the Keplerian model past 5R_e. Likewise, the mass function can be extrapolated, but not to the same precision as it can be interpolated. To add to the error in observational data, the spectrograph had a spatial resolution of only 4.16" (where the galaxy measures 20″), whereas Ferré-Mateu, et al. obtained a resolution of 1″, and calculated higher velocities (by ~30 km/s) and a higher mass (1.3 ± 0.3)×10^{11} $M_\odot$ (23).

Another source of uncertainty is the size of the over-massive black hole at the center of NG1277. Every star in NGC 1277 is older than 8 Gyr, therefore the black hole must be at least as old, as it is unlikely for a black hole to be accreted without star formation. In 2012, van den Bosch et al. presented an estimation of NGC 1277's black hole to be 59% of the mass of the galaxy's bulge (1.7×10^{10} $M_\odot$) (24) and the masses of the black holes are believed to correlate with properties of the host-galaxy bulge component. Several explanations have been proposed for the existence of these locally established empirical relationships, including the non-causal, statistical process of galaxy-galaxy merging, direct feedback between the black hole and its host galaxy, and galaxy-galaxy merging and the subsequent violent relaxation and dissipation. The empirical scaling relations are therefore important for distinguishing between various theoretical models of galaxy evolution, and they furthermore form the basis for all black-hole mass measurements at large distances. Observations have shown that the mass of the black hole is typically 0.1 per cent of the mass of the stellar bulge of the galaxy. Until now, the galaxy with the largest known fraction of its mass in its central black hole (11 per cent. While this would have obvious repercussions in studying the galaxy's matter distribution, it has since been re-estimated at 5×10^9 $M_\odot$, or about 3–4% of the galaxy's mass (25, 26). An affirmation made in the same article that the rotation curve of NGC 1277 stays flat out to five R_e clashes with our data and therefore questions this article's report on a normal dark matter halo (24). The level of uncertainty regarding the black hole mass adds a layer of complexity to any calculation of matter distribution being made.

Our use of rotation curves to calculate the mass of NGC 1277 could also be less reliable because the method assumes an infinitesimally thin disk, where velocities reflect the distribution of mass within the plane of the galaxy, but NGC 1277 is a thick, bulge-dominated lenticular galaxy in which significant mass lies outside the disk. Additional uncertainty arises from the inherent ambiguity of bulge-to-disk decomposition in lenticulars, which directly affects mass modeling (27–36). Warping, though a common source of error in spirals, can be ruled out for NGC 1277 given its highly uniform, edge-on structure (37–39).

A final source of error worth mentioning is related to the fact that NGC 1277 is a dispersion dominated galaxy, meaning it has a high velocity dispersion relative to its rotation speed, especially within the first R_e. The high velocity dispersions observed in the bulge of NGC 1277 are indicative of higher pressure support, which plays a role in supporting the galaxy against gravitational collapse, and would likely result in lower rotational velocities (40). The formula we used to derive enclosed mass given rotational velocities works well for rotating gas in spiral galaxies but less so for this type of galaxy, a compact galaxy with a large central bulge (as explained above). The use of a Virial mass estimator may have been a more straightforward way to estimate the mass for NGC 1277. In this theorem, the mass in the system relies similarly on its radius and the gravitational constant; however, instead of using the squared velocities, it is a function of the square of the velocity dispersion observed in the first R_e. This equation also includes a constant that is estimated based on specific morphological aspects of the system, such as its shape or density profile, which we cannot compute based solely on kinematic data. For example, in a spherical system, the standard proportionality factor applied to the Virial mass equation is 3; whereas. for a compact, high-dispersion galaxy like NGC 1277, a more appropriate factor is 5 (41) Given these uncertainties, we opted to apply a simplified rotation curve analysis to the dark matter deficient relic galaxy NGC 1277 using experimental kinematic data from the George and Cynthia Mitchell Spectrograph. By applying Kepler's third law, we fit the relationship between radii and mass to find a total mass of 5.8×10^{10} $M_\odot$ within 6 kpc, which is substantially lower than the 1.8×10^{11} $M_\odot$ reported in the literature for the same region (22).

This discrepancy highlights the limitations of relying on basic dynamical models. Throughout this paper's exploration of the rotation curve, as well as possible factors that influence the results given by it, we have concluded that estimations of mass distribution that consider only velocity measurements are likely to diverge from more accurate, model-informed results. Although rotation curves offer a logical and accessible starting point, especially when data or resources are limited, they cannot capture the full range of structural and dynamical features found in real galaxies.

Due to a lack of information about bulge concentrations, warps, precise black hole mass, percentage of dark matter and many other factors not determined by kinematics, the rudimentary rotation curve must be used alongside more advanced techniques, including Multi-Gaussian Expansion fitting and JAM models to achieve more accurate results. Nevertheless, with the growing observations of dark matter

https://doi.org/10.59720/25-050

deficient galaxies, rotation curves remain a valuable tool, offering a quick way to get a visual assessment of whether a galaxy has an unusual mass distribution, or an anomalous DMF.

Our next steps will be to apply this method to efficiently screen galaxies of varying age, size, and morphology for Keplerian-like rotation curves, with the broader goal of identifying new dark matter deficient candidates more rapidly and accessibly, prior to engaging in extensive modelling. We also aim to experiment with more complex galaxy models, incorporating new data from galaxies with interesting or suggestive rotation curves, and exploring how these inputs may necessitate further refinement of the models themselves. Unexpected cases, such as galaxies that appear to lack dark matter, may challenge our current understanding of galaxy dynamics, but they also offer valuable opportunities to adapt our models and revise or reject theories based on new observations.

Fritz Zwicky famously mentioned in 1937 that without taking into consideration additional information one cannot calculate galactic masses from observed rotations (1). We conclude that this statement stays true even when we take dark matter into account.

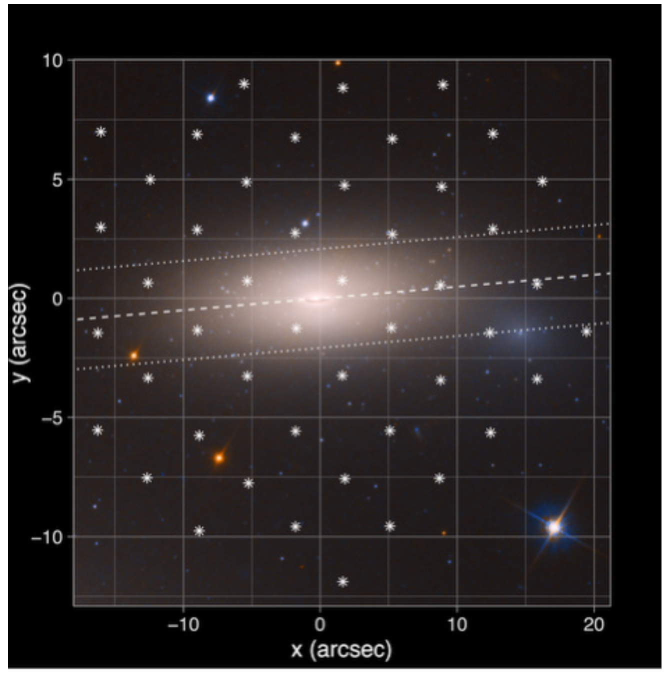

Figure 5: GCMS fiber selection. From the 47 GCMS fibers covering the field of view of NGC 1277 (asterisks), those with y values falling within 2.08” (dotted lines) of the kinematic major axis (PA 92.9) (dashed line) were selected for plotting the rotation curve (Figure 4). The estimated galactic center is located at the origin (0,0) and x,y coordinates are relative to the galactic center. The Hubble Space Telescope image of NGC 1277 was overlayed on the graph (48).

MATERIALS AND METHODS

Spectographic Fiber Selection

To plot the rotation curve for NGC 1277, we used a data table that provides the kinematics (22, 42). These data were extracted using the Penalized PiXel-Fitting (pPXF) method from the reduced spectra obtained from the George and Cynthia Mitchell Spectrograph (GCMS) on 29–31 Dec. 2019 for the Metal-THINGS program (43, 44). The field view of the GCMS instrument consists of a bundle of 246 optical fibers with a resolution of 4.16” (arcseconds) within the integral field unit (IFU) that transmit light from the telescope to the gratings in the spectrograph that split the light into separate wavelengths (3400–6850 Å with a resolution of 1–5.3 Å depending on the grating used) which are then detected on a 2048 × 2048 CCD camera (45). The VP1 grating (grism) with a 5.3 Å spectral resolution was used in this study (22). Additionally, a three-pointing dithering program was used to effectively increase the number of fiber readings from 246 to achieve 738 fiber coverage of the field of view. Observations taken in a 3-position dither pattern provide essentially complete coverage within a 100×10^2 arcsecond field of view. At the distance of NGC 1277, this corresponds to approximately 70 kpc with a resolution of about 1.4 kpc per fiber.

First, we selected the angular velocity data points based on their fibers’ corresponding spatial coordinates (Figure 5) and selected those whose fibers’ centers were within a restricted distance from the major axis (Table 1), determined to be at a position angle of 92.9˚ from the celestial north pole. This parameter is necessary for selecting fibers within the main disk of the galaxy, as these are the ones whose kinematic data, in terms of their horizontal component, will have the best correlation with the rotational velocity. For this value we chose 2.08”, which corresponds to the fiber radius in arcseconds.

Data transformation and error propagation

The kinematic data obtained was in terms of km/s with respect to the galaxy’s velocity, determined at 5097 km/s for NGC 1277, and therefore was in no need of additional transformation. No uncertainty was given for the velocity of the galaxy, but the kinematic data was already corrected for this velocity and we can assume any error was propagated and accounted for in the reported uncertainties for the kinematic data. However, we transformed the spatial data, consisting of x and y coordinates in arcseconds, to represent a radial distance (kpc) from the center of the galaxy.

First, we derived the distance (kpc) between each optical fiber and the center of the galaxy, from the arcsecond coordinates, by taking the tangent of the angles and multiplying by the distance to the galaxy, calculated to be 72.4 ± 1.0 Mpc. We found this distance by taking the mean of the co-moving (72.4 Mpc), luminosity (73.6 Mpc), and angular diameter distances (71.1 Mpc), where the error corresponds to the standard deviation (22).

Subsequently, we derived the radial distance from the coordinates, now in kpc, by using the Pythagorean theorem to find the hypotenuse of the x and y vectors from the center, with coordinates (0,0). The relative error for the radial distance is therefore 1.4%.

Correction of velocities for inclination angle

The kinematic data obtained from the fibers only considers the light received in the line of sight, taking the inclination angle of the galaxy to be exactly 90˚, i.e. edge-on. Using simple trigonometric properties, this would suggest that the horizontal component of the velocities, captured by the spectrograph, is equal to the vectors of the velocities, since dividing the two yields sin(i), which would be 1. However, the inclination angle of NGC 1277 is closer to i = 76˚ (22, 24). Therefore, we corrected reported velocities (corresponding only to the horizontal component) for i = 76° by dividing each by sin(76) to yield corrected vector velocities (indicated as v_{corr}) with higher magnitudes (Table 1). To propagate the error corresponding to the corrected velocities, we maintain the relative error by multiplying Δv/v times v_{corr}, which has the same effect as dividing the reported errors by sin(76) as we take the inclination to be a constant with no associated error.

Both the original velocities and those corrected for the inclination angle have been used to calculate the corresponding uncorrected and corrected masses (Table 1). Though correcting for inclination is an important factor in providing more accurate results, it only elevates measured velocities by a maximum of 7.6 km/s, reflecting a maximum rise in mass estimations of 0.3×10^{10} $M_\odot$ in the outer orbits, a value contained within the original mass uncertainties for larger radii. Uncertainty in the inclination angle itself would increase error in the mass, thereby allowing for a higher maximum value (and a lower minimum value) for the estimated mass, because larger inclination reflects higher velocities.

Dynamical mass estimation

Posing the galaxy as a rotating frame, the centripetal force is the inward force required to keep objects (stars, dust, gas, etc.) moving along a curved or circular path, always directed toward the center of the galaxy, while the gravitational force attracts the orbiting objects in the same direction, similarly altering the direction of their rotational velocity vector. Thus, we find the stable orbits which an object must complete according to its many variables by setting centripetal and gravitational forces equal to each other,

$$\frac{mv^2}{r} = \frac{GMm}{r^2} \qquad \text{(Equation 3)}$$

where (m) is the dynamical tracer mass (in this case, the group of stars within the field of a particular optic fiber of the GCMS IFU) orbiting around a total mass (M) enclosed within radius (r), G is the gravitational constant, and v is the rotational velocity of stars orbiting along the specified orbit of radius r. It is important to note that this calculation makes the approximation that most mass falls within the plane of the galaxy.

By simplifying the expression, solving for mass M,

$$M = \frac{rv^2}{G} \qquad \text{(Equation 4)}$$

the experimentally measured velocity and radius can be converted to a value for cumulative mass enclosed within that radius. As velocity is not constant, we determined the relationship between mass and any arbitrary radii by fitting a logarithmic function to the data points using the lm function in R v.4.4.2 and using the predict function with the new arbitrary series of r values. As the geometry of NGC 1277 is elliptical or lens-like with only a pseudobulge, this function fits the data well. The enclosed mass as a function of radius (M_r) was determined for different effective radii, where 1R_e is the radius within which half of the light of the galaxy is emitted and 5R_e is five times that radius.

Stellar mass estimation

To determine the total stellar mass using photometric data, we used the 13 surface brightness values from Comerón et al. Table A.1 obtained from a Hubble Space Telescope image (22). We computed the cumulative sum of the products of the average surface brightness and the annular areas between adjacent radii out to 5 kpc to derive a total luminosity of 2.1×10^{10} $L_\odot$. To determine the total stellar mass enclosed within 5 kpc, we multiplied the total luminosity by the published M/L of 6.5 (the M/L scale is relative to that of the sun, which is defined to be 1) (46).

Under some specific assumptions about the galaxy's geometry, symmetry, and stellar motion, which may or may not hold in the case of NGC 1277, the discrepancy between total mass determined using the rotation curve and the sum of all the masses of the stars within the galaxy (or luminous matter) and the central black hole can then be used to estimate the fraction of dark matter making up the galaxy.

ACKNOWLEDGMENTS

We would like to thank the Joves i Ciència program and to Fundació La Pedrera for making this experience possible. We would also like to acknowledge Gina Alioto and Roger Dalmau for taking the time to review the manuscript as well as Sébastien Comerón for his professional and useful explanations regarding his article, "The massive relic galaxy NGC 1277 is dark matter deficient."

Received: March 1, 2025
Accepted: July 17, 2025
Published: October 7, 2025

REFERENCES

1. Zwicky, Fritz. "On the Masses of Nebulae and of Clusters of Nebulae". Astrophysical Journal, vol. 86, 1937, pp. 217–246, doi:10.1086/143759.
2. Rubin, V. C. et al. "Extended rotation curves of high-luminosity spiral galaxies. IV - Systematic dynamical properties, SA through SC". The Astrophysical Journal, vol. 225, Nov. 1978, pp. L107, doi:10.1086/182804.
3. Slipher, V. M. "The detection of nebular rotation". Lowell Observatory Bulletin, vol. 2, pp.66-66, 1914, https://articles.adsabs.harvard.edu/pdf/1914LowOB...2...66S
4. Pease, F. G. "The rotation and radial velocity of the central part of the andromeda nebula." Proceedings of the National Academy of Sciences of the United States of America, vol. 4, no. 1, Jan. 1918, pp. 21–24, doi:10.1073/pnas.4.1.21.
5. Oort, Jan H. "The force exerted by the stellar system in the direction perpendicular to the galactic plane and some related problems". Bulletin of the Astronomical Institutes of the Netherlands, vol. 6, 1932, pp. 249–287.
6. Babcock, Horace W. "The rotation of the Andromeda Nebula". Lick Observatory Bulletin, vol. 19, no. 498, 1939, pp. 41–51.
7. Bertone, Gianfranco et al. "History of dark matter". Reviews of Modern Physics, vol. 90, no. 4, 15th Oct. 2018, pp. 045002, doi:10.1103/RevModPhys.90.045002.
8. Zwicky, F. "Die Rotverschiebung von extragalaktischen Nebeln". Helvetica Physica Acta, vol. 6, 1st Jan. 1933, pp. 110–127, doi:10.48550/arXiv.1711.01693.
9. Roberts, M. S. et al. "The rotation curve and geometry of M 31 at large galactocentric distances." The Astrophysical Journal, vol. 201, Oct. 1975, pp. 327, doi:10.1086/153889.
10. Pauli, Wolfgang. "Pauli letter collection: Letter to Lise Meitner". https://cds.cern.ch/record/83282/.
11. Cowsik, R. et al. "Gravity of Neutrinos of Nonzero Mass in

Astrophysics". The Astrophysical Journal, vol. 180, Feb. 1973, pp. 7, doi:10.1086/151937.
12. Bernardini, Gilberto. "The Program of Neutrino Experiments at CERN". In Proceedings of the 1960 Rochester Conference, 1960.
13. Hasert, F. J. et al. "Observation of neutrino-like interactions without muon or electron in the gargamelle neutrino experiment". Physics Letters B, vol. 46, no. 1, 1973, pp. 138–140, doi: 10.1016/0370-2693(73)90499-1.
14. Wilczek, F. "Problem of Strong P and T Invariance in the Presence of Instantons". Phys. Rev. Lett., vol. 40, no. 5, Jan. 1978, pp. 279–282, doi:10.1103/PhysRevLett.40.279.
15. Weinberg, Steven. "A New Light Boson?" Phys. Rev. Lett., vol. 40, no. 4, Jan. 1978, pp. 223–226, doi:10.1103/PhysRevLett.40.223.
16. Milsztajn, A. et al. "Not enough stellar mass machos in the galactic halo". Nuclear Physics B - Proceedings Supplements, vol. 91, no. 1–3, Jan. 2001, pp. 413–419, doi:10.1016/S0920-5632(00)00970-1.
17. Buzzo, Maria Luisa et al. "A new class of dark matter-free dwarf galaxies?: I. Clues from FCC 224, NGC 1052-DF2, and NGC 1052-DF4". Astronomy & Astrophysics, vol. 695, Mar. 2025, pp. A124, doi:10.1051/0004-6361/202453522.
18. van Dokkum, Pieter et al. "A galaxy lacking dark matter". Nature, vol. 555, no. 7698, Mar. 2018, pp. 629–632, doi:10.1038/nature25767.
19. Tortora, C. et al. "Nature versus nurture: relic nature and environment of the most massive passive galaxies at z < 0.5". Astronomy & Astrophysics, vol. 638, Jun. 2020, pp. L11, doi:10.1051/0004-6361/202038373.
20. Lapiner, Sharon et al. "Wet compaction to a blue nugget: a critical phase in galaxy evolution". Monthly Notices of the Royal Astronomical Society, vol. 522, no. 3, 2nd May 2023, pp. 4515–4547, doi:10.1093/mnras/stad1263.
21. Keim, Michael A. et al. "Tidal Distortions in NGC1052-DF2 and NGC1052-DF4: Independent Evidence for a Lack of Dark Matter". The Astrophysical Journal, vol. 935, no. 2, 1st Aug. 2022, pp. 160, doi:10.3847/1538-4357/ac7dab.
22. Comerón, Sébastien et al. "The massive relic galaxy NGC 1277 is dark matter deficient". Astronomy & Astrophysics, vol. 675, Jul. 2023, pp. A143, doi:10.1051/0004-6361/202346291.
23. Ferré-Mateu, Anna et al. "Two new confirmed massive relic galaxies: red nuggets in the present-day Universe". Monthly Notices of the Royal Astronomical Society, 2017, doi: 10.1093/mnras/stx171.
24. van den Bosch, Remco C. E. et al. "An over-massive black hole in the compact lenticular galaxy NGC 1277." Nature, vol. 491, no. 7426, 29th Nov. 2012, pp. 729–731, doi:10.1038/nature11592.
25. Walsh, Jonelle L. et al. "A 5 × 109 $M_\odot$ BLACK HOLE IN NGC 1277 FROM ADAPTIVE OPTICS SPECTROSCOPY". The Astrophysical Journal, vol. 817, no. 1, 18th Jan. 2016, pp. 2, doi:10.3847/0004-637X/817/1/2.
26. Krajnović, Davor et al. "A quartet of black holes and a missing duo: probing the low end of the MBH–sigma relation with the adaptive optics assisted integral-field spectroscopy". Monthly notices of the Royal Astronomical Society, vol. 477, no. 3, 1st Jul. 2018, pp. 3030–3064, doi:10.1093/mnras/sty778.
27. Gunn, James E. et al. "On the infall of matter into clusters of galaxies and some effects on their evolution". The Astrophysical Journal, vol. 176, Aug. 1972, pp. 1, doi:10.1086/151605.
28. Larson, R. B. et al. "The evolution of disk galaxies and the origin of S0 galaxies". The Astrophysical Journal, vol. 237, May 1980, pp. 692, doi:10.1086/157917.
29. Bekki, Kenji et al. "Passive Spiral Formation from Halo Gas Starvation: Gradual Transformation into S0s". The Astrophysical Journal, vol. 577, no. 2, Oct. 2002, pp. 651–657, doi:10.1086/342221.
30. Moore, Ben et al. "On the Destruction and Overmerging of Dark Halos in Dissipationless N-Body Simulations". The Astrophysical Journal, vol. 457, Feb. 1996, pp. 455, doi:10.1086/176745.
31. Moore, Ben et al. "Morphological Transformation from Galaxy Harassment". The Astrophysical Journal, vol. 495, no. 1, Mar. 1998, pp. 139–151, doi:10.1086/305264.
32. Moore, Ben et al. "Dark Matter Substructure within Galactic Halos". The Astrophysical journal, vol. 524, no. 1, 10th Oct. 1999, pp. L19–L22, doi:10.1086/312287.
33. Merritt, D. "Relaxation and tidal stripping in rich clusters of galaxies. II - Evolution of the luminosity distribution". The Astrophysical Journal, vol. 276, Jan. 1984, pp. 26, doi:10.1086/161590.
34. Miller, L. "Heating and cooling in clusters of galaxies". Monthly notices of the Royal Astronomical Society, vol. 220, no. 3, 1st Jun. 1986, pp. 713–722, doi:10.1093/mnras/220.3.713.
35. Byrd, Gene et al. "Tidal generation of active spirals and S0 galaxies by rich clusters". The Astrophysical Journal, vol. 350, Feb. 1990, pp. 89, doi:10.1086/168362.
36. Shelest, A. et al. "From spirals to lenticulars: Evidence from the rotation curves and mass models of three early-type galaxies". Astronomy & Astrophysics, vol. 641, Sep. 2020, pp. A31, doi:10.1051/0004-6361/202038184.
37. Burke, Bernard F. "Systematic distortion of the outer regions of the galaxy." The Astronomical journal, vol. 62, May 1957, pp. 90, doi:10.1086/107463.
38. Wakker, B. P. et al. "HIGH-VELOCITY CLOUDS". Annual review of astronomy and astrophysics, vol. 35, no. 1, Sep. 1997, pp. 217–266, doi:10.1146/annurev.astro.35.1.217.
39. Casertano, Stefano et al. eds. "Warped disks and inclined rings around galaxies". Cambridge University Press, Cambridge, England, 30th May 1991.
40. Dalcanton, Julianne J. et al. "PRESSURE SUPPORT IN GALAXY DISKS: IMPACT ON ROTATION CURVES AND DARK MATTER DENSITY PROFILES". The Astrophysical Journal, vol. 721, no. 1, 20th Sep. 2010, pp. 547–561, doi:10.1088/0004-637X/721/1/547.
41. Wel, Arjen Van Der et al. "The Mass Scale of High-redshift Galaxies: Virial Mass Estimates Calibrated with Stellar Dynamical Models from LEGA-C". The Astrophysical Journal, vol. 936, no. 1, 1st Sep. 2022, pp. 9, doi:10.3847/1538-4357/ac83c5.
42. Comerón, S. et al. "NGC1277 + NGC1278 spectra + kinematic information". doi:10.26093/cds/vizier.36750143.
43. Cappellari, Michele. "Full spectrum fitting with photometry in ppxf : stellar population versus dynamical masses, non-parametric star formation history and metallicity for 3200 LEGA-C galaxies at redshift z ≈ 0.8". Monthly Notices of the Royal Astronomical Society, vol. 526, no. 3, 10th Oct. 2023, pp. 3273–3300, doi:10.1093/mnras/stad2597.

https://doi.org/10.59720/25-050

44. Lara-López, M. A. et al. “Metal-THINGS: Association and optical characterization of supernova remnants with H I holes in NGC 6946”. Astronomy & Astrophysics, vol. 669, Jan. 2023, pp. A25, doi:10.1051/0004-6361/202245068.
45. “George and Cynthia Mitchell Spectrograph (GCMS) | McDonald Observatory”. https://mcdonald.utexas.edu/research-facilities/HJST/gcms, Accessed 29 June 2025.
46. Yıldırım, Akın et al. “MRK 1216 and NGC 1277 – an orbit-based dynamical analysis of compact, high-velocity dispersion galaxies”. Monthly Notices of the Royal Astronomical Society, vol. 452, no. 2, 11th Sep. 2015, pp. 1792–1816, doi:10.1093/mnras/stv1381.
47. “Galaxy NGC 1277 - NASA Science”. https://science.nasa.gov/asset/hubble/galaxy-ngc-1277/, Accessed 7 September 2025.
48. Beasley, Michael A. et al. “A single population of red globular clusters around the massive compact galaxy NGC 1277”. Nature, vol. 555, no. 7697, Mar. 2018, pp. 483–486, doi:10.1038/nature25756.